ACS Photonics

Article

pubs.acs.org/journal/apchd5

Lasing Action with Gold Nanorod Hyperbolic Metamaterials

Rohith Chandrasekar,[†] Zhuoxian Wang,[†] Xiangeng Meng,*[,†] Shaimaa I. Azzam,[†] Mikhail Y. Shalaginov,[†] Alexei Lagutchev,[†] Young L. Kim,[‡] Alexander Wei,[§] Alexander V. Kildishev,[†] Alexandra Boltasseva,[†] and Vladimir M. Shalaev*[,†]

[†]School of Electrical and Computer Engineering and Birck Nanotechnology Center, [‡]Weldon School of Biomedical Engineering, and [§]Department of Chemistry, Purdue University, West Lafayette, Indiana 47907, United States

Supporting Information

ABSTRACT: Coherent nanoscale photon sources are of paramount importance to achieving all-optical communication. Several nanolasers smaller than the diffraction limit have been theoretically proposed and experimentally demonstrated using plasmonic cavities to confine optical fields. Such compact cavities exhibit a strong Purcell effect, thereby enhancing spontaneous emission, which feeds into the lasing modes. However, most plasmonic nanolasers reported so far have employed relatively narrowband resonant nanostructures and therefore had the lasing restricted to the proximity of the resonance wavelength. Here, we report on an approach based on gold nanorod hyperbolic metamaterials for lasing. Hyperbolic metamaterials provide broadband Purcell enhancement due to the large photonic density of optical states, while also supporting surface plasmon modes to deliver optical feedback for lasing due to nonlocal effects in nanorod media. We experimentally demonstrate the advantage of hyperbolic metamaterials in achieving lasing action by its comparison with that obtained in a metamaterial with elliptic dispersion. The conclusions from the experimental results are supported with numerical simulations comparing the Purcell factors, surface plasmon modes, and spontaneous emission factors for the metamaterials with different dispersions. We show that although the metamaterials of both types support lasing, emission with hyperbolic samples is about twice as strong with 35% lower threshold versus the elliptic ones. Hence, hyperbolic metamaterials can serve as a convenient platform of choice for nanoscale coherent photon sources in a broad wavelength range.

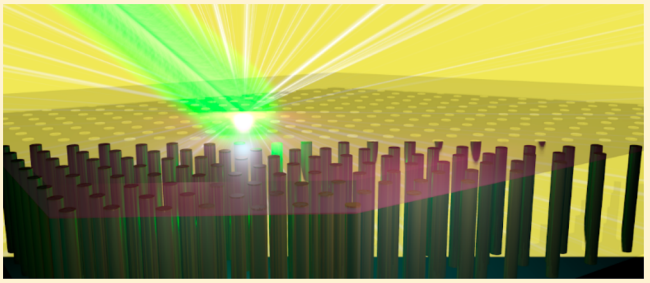

KEYWORDS: *hyperbolic metamaterial, metal nanorods, nanolasers, Purcell enhancement, nonlocal effect*

Since its invention in 1960,[1] the laser has seen tremendous developments and has quickly revolutionized fundamental and applied fields such as metrology, medicine, data storage, fabrication, and telecommunications, among others.[2] With the ever-growing need for data transfer speeds and compact devices, considerable efforts have been made toward miniaturizing the laser for on-chip integration.[3−7] While photonic cavities have proven to exhibit high-Q factors enabling strong lasing, their miniaturization to the nanoscale is not viable since the diffraction limit requires the cavity length to be at least half the lasing wavelength.[8−10] In contrast, plasmonic cavities, which can be employed to achieve optical amplification and lasing action with charge oscillations, have successfully led to the design of coherent photon sources no longer limited by the diffraction limit.[10] Coupling of emitters with the strongly confined electromagnetic fields associated with plasmonic oscillations can significantly enhance spontaneous emission, a process known as the Purcell effect.[11] This effect yields a redistribution of spontaneous emission over wavevector space (k-space), resulting in light being preferentially coupled to the lasing modes.[12]

Several plasmonic lasers have already been demonstrated using various geometries, such as semiconductor−dielectric−metal hybrid cavities,[7] metal−insulator−metal waveguides,[13] whispering gallery cavities,[14] core−shell particles,[15,16] and nanohole/particle arrays.[17−19] These methods generally used geometries with strong cavity resonances to gain Purcell enhancement and hence lasing as described above. The Purcell enhancement arising from the resonance of metallic structures usually exhibits a relatively narrow bandwidth, thus restraining the achievable lasing frequency. An alternative approach to realize Purcell enhancement is based on structures with broadband responses, which can be achieved by engineering the dispersion of metamaterials.[20−22] In this work, we report on the use of nanorod-based metamaterials with hyperbolic and elliptic dispersion, namely, a hyperbolic metamaterial (HMM) and an elliptic metamaterial (EMM), to achieve lasing. Our nanorod-based metamaterials are composed of vertically aligned gold nanorods coated with a poly(vinyl alcohol) (PVA) film embedded with rhodamine 101 (R101) dye

Received: January 5, 2017
Published: February 16, 2017

DOI: 10.1021/acsphotonics.7b00010
ACS Photonics 2017, 4, 674−680

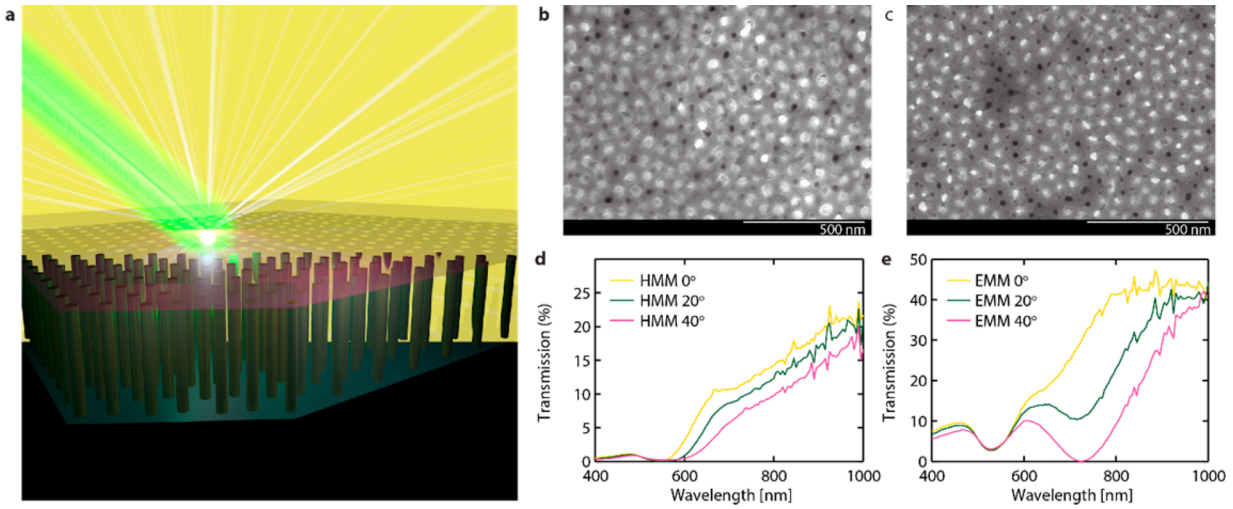

Figure 1. (a) Scheme of lasing action from nanorod-based metamaterials. (b, c) Top-view SEM images of HMM and EMM, with metal fill ratios of 35% and 14%, respectively. (d, e) Transmission spectra of HMM and EMM illuminated with TM-polarized light at 0°, 20°, and 40° incidence.

molecules. The dispersion of a given metamaterial can be controlled by changing the fill ratio of the metal.[23] Our experimental results show that an HMM exhibits a larger enhancement of lasing over an EMM, which could be related to both Purcell enhancement and field coupling to surface plasmon modes due to nonlocal effects in the nanorod structure. Our simulations show that an HMM gives a larger magnitude of Purcell enhancement than an EMM, which could feed a higher portion of spontaneous emission into the lasing mode. Concurrently, simulations indicate that nonlocal effects give rise to a more profound resonance in an HMM, which should favor the formation of optical feedback for lasing. Due to both of these effects, nanorod-based HMMs could serve as a competitive platform for lasing at the nanoscale. Furthermore, the nanorod-based metamaterials by virtue of their broadband response could be integrated with a wide range of optical gain media to achieve lasing at a desired frequency.

HMMs are a special class of highly anisotropic metamaterials with effective dielectric permittivities of opposite signs for orthogonal tensor components,[24−28] as shown in eq 1. Longitudinal and transverse effective permittivities, $\varepsilon_{\perp}$ and $\varepsilon_{\parallel}$, can be calculated using the Maxwell−Garnett effective medium theory,[29] as shown in eqs 2 and 3,

$$\varepsilon = \begin{pmatrix} \varepsilon_{\parallel} & 0 & 0 \\ 0 & \varepsilon_{\parallel} & 0 \\ 0 & 0 & \varepsilon_{\perp} \end{pmatrix} \tag{1}$$

$$\varepsilon_{\parallel} = \varepsilon_{\mathrm{d}}\left[\frac{\varepsilon_{\mathrm{m}}(1+f)+\varepsilon_{\mathrm{d}}(1-f)}{\varepsilon_{\mathrm{m}}(1-f)+\varepsilon_{\mathrm{d}}(1+f)}\right] \tag{2}$$

$$\varepsilon_{\perp} = f\varepsilon_{\mathrm{m}} + (1-f)\varepsilon_{\mathrm{d}} \tag{3}$$

where ε_{m} and ε_{d} are permittivities of metal and dielectric materials, respectively, comprising the metamaterial, and f is the metal fill ratio.

So far two types of HMMs have been classified. Type-I HMMs are typically based on aligned nanowire/nanorod arrays having $\varepsilon_{\perp} < 0$ and $\varepsilon_{\parallel} > 0$,[23,30−37] whereas type-II HMMs are based on metal−dielectric stacks with $\varepsilon_{\perp} > 0$ and $\varepsilon_{\parallel} < 0$.[27,38−40] By adjusting the chemical composition of the metamaterial or the metal fill ratio, the dispersion of the metamaterial can be tuned from elliptic to hyperbolic. It has been shown that metamaterials exhibiting hyperbolic properties can support unique optical waves with very small or large mode indices, allowing for stronger light−matter interaction.[32,33] Furthermore, the fields in the nanorod metamaterial can exhibit strong spatial variation, yielding a nonlocal response.[32,41]

Several physical phenomena have already been demonstrated either theoretically[42−44] or experimentally[21,22,45−52] with HMMs, such as focusing,[42] subdiffraction imaging,[45] thermal emission enhancement,[43,46] and spontaneous emission enhancement.[21,22,44,47−52] HMMs exhibit large Purcell enhancement due to the singularity in their local density of optical states (LDOS), a property that results from hyperbolic dispersion.[20,48] Radiative decay rate enhancement of emitters such as dyes and nitrogen-vacancy centers using HMMs has been studied extensively,[22,23,47−53] with as high as 76-fold enhancement of the spontaneous emission rate being reported.[22] On the other hand, it has been shown that the Purcell effect could contribute to efficient optical amplification and lasing action, provided that a portion of the enhanced spontaneous emission feeds into the lasing mode.[12] To our knowledge, so far there was only one report that addressed the possibility to achieve stimulated emission from an HMM composed of Ag and MgF_2 layer stacks.[53] Although a reduced threshold was observed in an HMM when compared to a reference device based on a bare Ag film, the emission efficiency from the HMM was notably lower than the latter. Thus, the full potential of an HMM to achieve lasing with low threshold and high efficiency needs to be explored further.

In this work, two gold nanorod arrays embedded in anodic alumina templates have been fabricated, exhibiting hyperbolic (labeled HMM) and elliptic dispersion (labeled EMM) at the emission wavelength of R101 (λ = 606 nm), according to local effective medium theory (EMT; see eqs 1−3). The different dispersion characteristics were achieved by altering the metal fill ratio using different nanorod diameters (Supporting Information S1).

Arrays of gold nanorods were fabricated by electrodeposition within nanoporous aluminum oxide membranes that were prepared by the anodization of Al films deposited on tantalum pentoxide and Au-coated glass substrates in 0.3 M H_2SO_4

DOI: 10.1021/acsphotonics.7b00010
ACS Photonics 2017, 4, 674−680

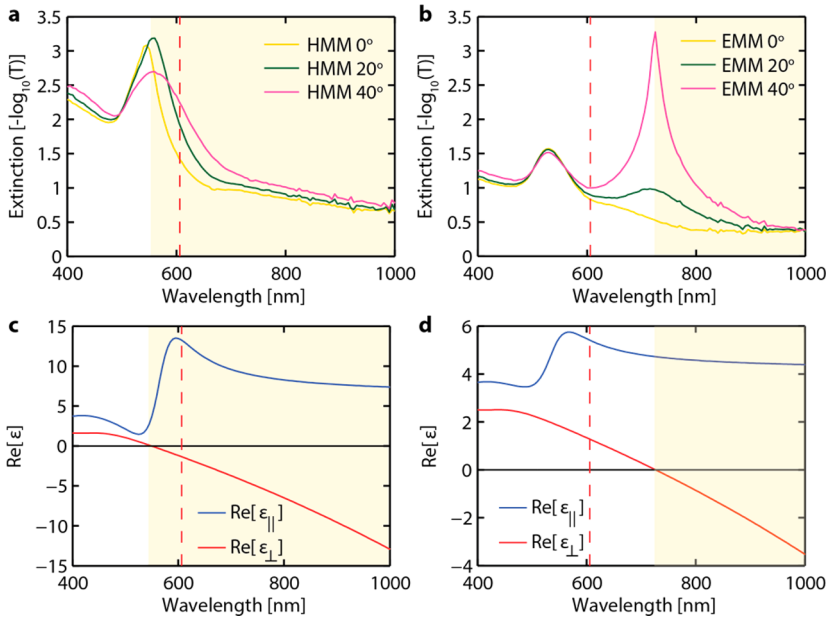

Figure 2. (a, b) Experimental extinction spectra for an HMM (a) and an EMM (b). (c, d) Effective anisotropic permittivities of an HMM (c) and an EMM (d) estimated using Maxwell−Garnett theory. Shaded regions indicate wavelength range where the metamaterial exhibits hyperbolic type-I dispersion. Dashed red line indicates the central emission wavelength of the R101 dye (606 nm).

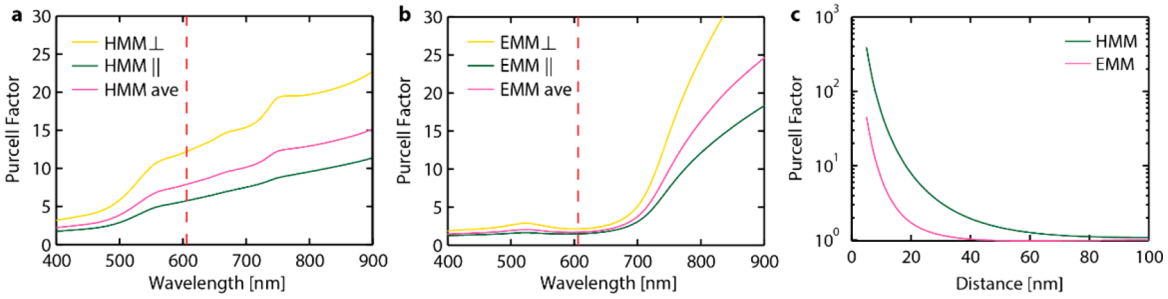

Figure 3. Theoretical estimations of the Purcell factor versus emission wavelength for a dipole located 20 nm above an HMM (a) and an EMM (b), as well as dependence of the Purcell factor on the distance of the dipole from the metamaterial surface (c) at the central emission wavelength of R101 (606 nm, indicated with a red dashed line in (a) and (b)). Yellow, green, and pink curves in (a) and (b) refer to dipoles oriented perpendicular and parallel to the metamaterial surface and averaged, respectively. The Purcell factor in (c) is plotted for the averaged dipole orientation.

(Supporting Information S1). Anodization was performed at 30 V for the HMM and at 25 V for the EMM, to yield approximate pore diameters of 40 ± 2 and 25 ± 2.5 nm, respectively, surface densities of 35% and 14%, respectively, and nanopore heights of 250 nm. Gold nanorods were electrodeposited according to the previously described procedure under galvanostatic conditions[54,55] using a current density of 0.5 mA/cm^2, with constant electrodeposition up to the maximum height allowed by the nanoporous alumina templates, at which point a distinct drop in voltage (>20%) was observed. SEM images of the nanorod-based HMM and EMM indicate that the nanorods have uniform diameters and are well dispersed within the Al_2O_3 matrix, which has an approximate pore-to-pore distance of 60 nm for each sample (Figure 1b,c).

Transmission spectra using TM-polarized light at different angles of incidence show that the HMM sample exhibits complete extinction up to 550 nm, whereas the EMM sample exhibits transmission minima at 530 and 710 nm (Figure 1d,e). These minima can be assigned to the epsilon-near-pole (ENP, $\varepsilon_{\parallel} \rightarrow \infty$) and epsilon-near-zero (ENZ, $\varepsilon_{\perp} = 0$) resonances, where the ENZ response (and subsequent cutoff wavelength for hyperbolic dispersion) can be tuned easily by adjusting the fill ratio.[56] In the case of an HMM, only one resonance band is observed since the ENP and ENZ responses overlap starting at λ = 530 nm, whereas the EMM has distinct ENP (λ = 530 nm) and ENZ (λ = 710 nm) responses, as seen in Figure 2a,b. Simulations of the optical responses of the HMM and EMM structures also match the experimental extinction data (Supporting Information S2); effective Maxwell−Garnett permittivities were calculated based on the fill ratios for each sample and the permittivity values of bulk Au and amorphous Al_2O_3 (Figure 2c,d). Both the extinction and permittivity plots show that the HMM exhibits hyperbolic dispersion and the EMM exhibits elliptic dispersion at the central emission wavelength of R101 (606 nm). In addition, we have calculated the isofrequency curves for both HMMs and EMMs based on the effective medium permittivities (Supporting Information S3), which confirms the hyperbolic and elliptic dispersion at 606 nm, respectively.

The Purcell factor, F_P, is defined as the ratio of the total decay rate from a dipole source situated in an enhancing medium, such as a cavity, to that in the bulk dielectric (PVA in this case). HMMs, due to their singularity in LDOS, offer a nonresonant method of achieving large Purcell factors for

DOI: 10.1021/acsphotonics.7b00010
ACS Photonics 2017, 4, 674−680

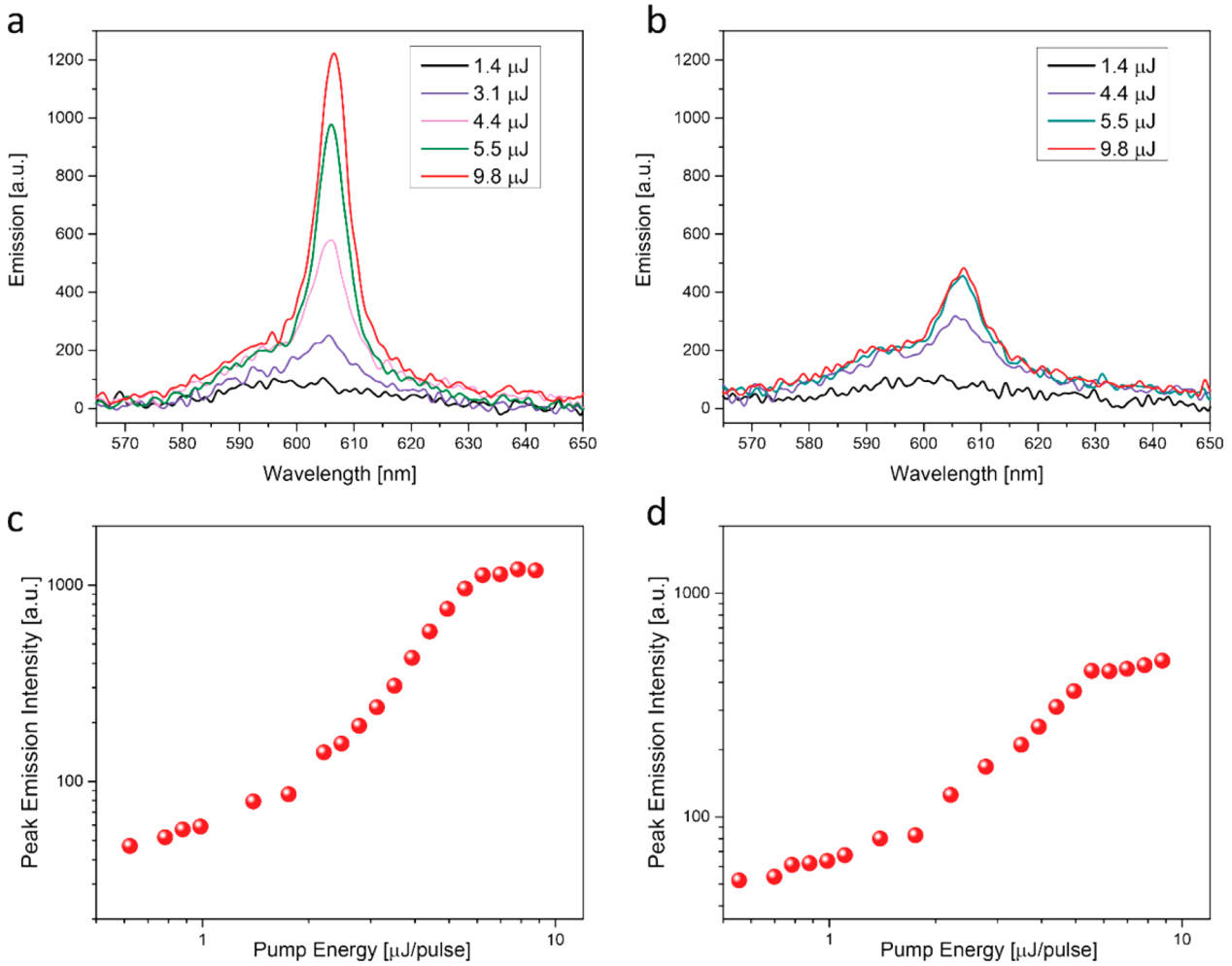

Figure 4. (a, b) Emission spectra recorded under various pump energies for an HMM (a) and EMM (b). (c, d) Log−log scale plots of peak emission intensity as a function of pump energy for the HMM (c) and EMM (d), where the slopes change from spontaneous emission to lasing.

emitters.[48] We estimated the Purcell factors for our HMM and EMM structures by simulating the coupling of dipole emitters with our metamaterials, defined by local EMT. Using the standard Green's function formalism,[57] we calculated the Purcell factors for a dipole embedded in PVA (refractive index n = 1.5) placed 20 nm above an HMM and an EMM supported on glass substrates (n = 1.5), as shown in Figure 3a and b. In the calculation, the polarization of the dipole is addressed as well. The calculation results show that the HMM provides a Purcell factor of 5.75 for a dipole parallel to the HMM surface and 12.21 for a dipole perpendicular to the surface at the central emission wavelength of R101 (λ = 606 nm). On the other hand, the EMM provides a Purcell factor of 1.5 and 2.15 for parallel and perpendicular orientations, respectively. On average the HMM provides an enhancement of 4.6 times over the EMM. The calculation also shows that the Purcell factor strongly depends on the distance of the dipole from the metamaterial surface (Figure 3c). For dipoles very close to the metamaterial surface (~5 nm), the Purcell factor for the HMM is extremely large, reaching up to 400, while the EMM provides an enhancement of only 46. As the dipole is moved away from the surface, the Purcell factor for the EMM decays much faster than that for the HMM, reaching ~1 within a 40 nm distance, while it is still slightly larger than 1 for the HMM at a distance of 100 nm. The k-space dissipated power density is further calculated in Supporting Information S4 to better explain the Purcell enhancement in the HMM and EMM structures.

The nanorod arrays were coated with a ~2 μm thick film of PVA embedded with R101 dye (10 mM). A frequency-doubled Nd:YAG picosecond laser (λ = 532 nm, pulse width = 400 ps, repetition rate = 1 Hz) was used to pump the samples. The emission from the samples was collected with a fiber, which was fed to a spectrometer equipped with a charge-coupled device (Supporting Information S5). Figure 4a,b shows the evolution of the emission spectra with the pump energy for both the HMM and EMM. Obvious spectral narrowing was observed for both the HMM and EMM when the pump energy was increased up to ~3.2 and 4.0 μJ, respectively. The full widths at half-maximum (fwhm) of the emission spectra from HMM and EMM samples were reduced to ~6 nm when the samples were pumped above respective thresholds (Supporting Information S6). The emission line width for both the HMM and EMM was found to be similar to those demonstrated in many other reports using laser dyes as gain media.[15,58] At a pump energy of ~9.8 μJ, the emission intensity from the HMM was twice as strong as that from the EMM. From the log−log scale plot of pump-dependent peak emission intensity (Figure 4c,d), we can see a clear threshold behavior for the two systems, as the slopes change from spontaneous emission to lasing. We have examined the threshold behavior at 5 points on each sample and found that the HMM achieved an average of 35% reduction

DOI: 10.1021/acsphotonics.7b00010
ACS Photonics 2017, 4, 674−680

in threshold energy compared to the EMM (Supporting Information S7).

As control samples, we have studied the emissions from a bare glass substrate and a 250 nm thick gold film, both coated with R101 in PVA (Supporting Information S8). Both samples show only spontaneous emission, without any noticeable spectral narrowing. We have also fabricated a lamellar HMM with 10 alternating layers of Au (8.9 nm) and Al_2O_3 (16.1 nm), which has the same metal fill ratio as the nanorod-based HMM. We applied the gain medium and conducted lasing measurements in the same way as described above; however, no lasing was observed before the sample was damaged by the pump pulse (Supporting Information S9). Therefore, the nanorod-based HMM provides a significant enhancement over its lamellar counterpart, exhibiting low-threshold lasing action.

As described above, the HMM exhibits a higher Purcell factor at the lasing wavelength compared to the EMM, which could partially account for low-threshold behavior observed in the HMM due to spontaneous emission being fed into the lasing mode. To further understand the lasing mechanism, we have computed optical responses and field distributions of the nanorod metamaterials (Supporting Information S10). In comparison to the EMM, the HMM exhibits a more distinguishable resonance arising from nonlocal effects,[32] as seen in the optical absorption spectrum (Figure S10c,d), and a higher magnitude of averaged local fields (Figure S10e,f) at ~606 nm. Along with a higher Purcell factor, the stronger resonance and local fields exhibited in the HMM could provide stronger feedback for lasing and thus lead to a lower threshold. The lasing behavior is further confirmed by simulations based on the finite-difference time-domain (FDTD) method (Supporting Information S11). Both spectral narrowing and the S-shaped dependence of the emission intensity on the pump energy were observed for our HMM and EMM laser devices. The simulation results are then fitted with the rate equations, leading to a β factor of 0.23 for the HMM and 0.08 for the EMM. The larger magnitude of the β factor in the HMM indicates that a larger portion of spontaneous emission is coupled to the lasing mode and results in a lower lasing threshold. Even though the experimental S-shaped plots in Figure 4c,d are imperfect due to the degradation of organic dyes at very high pump energies,[59−61] we believe that lasing occurred in our systems based on the agreement between experimental observations and numerical simulations. In contrast to the nanorod HMM, bare metal film and lamellar HMMs provide Purcell enhancement to some extent, but lack the resonant behavior needed to serve as feedback for lasing action.

It is noteworthy that the lasing herein is distinct from that reported in a previous work based on tilted silver nanorods in terms of sample configuration and lasing mode dispersion.[62] In ref 62, the tilted nanorods, acting as random scatterers, have relatively large distributions in both length and diameter. The dyes are infiltrated into the random nanorod arrays where significant scattering is naturally anticipated. In contrast, in this work the dyes are accumulated atop a relatively smooth metamaterial surface, so light scattering can be neglected. In addition, the features of lasing spectra in ref 62 are consistent with the behavior exhibited in random lasers with coherent feedback[63] and thus are distinct from the observations in this work.

In conclusion, we have demonstrated lasing action in metamaterials based on gold nanorod arrays coated with thin films of PVA embedded with R101, which can be tuned to exhibit hyperbolic or elliptic dispersion based on their metal fill ratio. Both metamaterials support lasing action, with emission from the HMM sample being twice as strong as that from the EMM sample while also exhibiting a 35% lower threshold. One interesting direction for future study is to infuse dyes directly into the matrix of the nanorod-based HMM, which would greatly enhance the emitter−field coupling and consequently give much lower thresholds for lasing. The HMM achieves broadband Purcell enhancement, suggesting its application as a source for coherent photon emission and Forster energy transfer[64] in a broad wavelength range.

■ ASSOCIATED CONTENT

Supporting Information

The Supporting Information is available free of charge on the ACS Publications website at DOI: 10.1021/acsphotonics.7b00010.

Fabrication and characterization details, simulated extinction spectra of nanorod-based metamaterials, isofrequency curves for metamaterials, equations for calculating the *k*-space dissipated power density, spectra narrowing and threshold distribution for nanorod HMM and EMM, emission from glass, gold film, and lamellar hyperbolic metamaterial samples, local field distributions, and loss compensation of plasmonic resonance in an HMM (PDF)

■ AUTHOR INFORMATION

Corresponding Authors

*E-mail (X. Meng): mengxiangeng@gmail.com.
*E-mail (V. M. Shalaev): shalaev@purdue.edu.

ORCID

Rohith Chandrasekar: 0000-0003-2785-1182
Zhuoxian Wang: 0000-0002-1299-7384

Author Contributions

R. Chandrasekar and Z. Wang contributed equally to this work.

Notes

The authors declare no competing financial interest.

■ ACKNOWLEDGMENTS

The authors acknowledge support from the Office of Naval Research grant (N00014-13-1-0649) and the Air Force Office of Scientific Research grant (FA9550-12-1-0024).

■ REFERENCES

(1) Maiman, T. H. Stimulated optical radiation in ruby. *Nature* **1960**, *187*, 493−493.

(2) Thyagarajan, K.; Ghatak, A. *Lasers: Fundamentals and Applications*, 2nd ed.; Springer, 2010.

(3) Lu, Y.-J.; Kim, J.; Chen, H.-Y.; Wu, C.; Dabidian, N.; Sanders, C. E.; Wang, C.-Y.; Lu, M.-Y.; Li, B.-H.; Qiu, X. Plasmonic nanolaser using epitaxially grown silver film. *Science* **2012**, *337*, 450−453.

(4) Ma, R. M.; Oulton, R. F.; Sorger, V. J.; Bartal, G.; Zhang, X. A. Room-temperature sub-diffraction-limited plasmon laser by total internal reflection. *Nat. Mater.* **2011**, *10*, 110−113.

(5) Wu, S. F.; Buckley, S.; Schaibley, J. R.; Feng, L. F.; Yan, J. Q.; Mandrus, D. G.; Hatami, F.; Yao, W.; Vuckovic, J.; Majumdar, A.; Xu, X. D. Monolayer semiconductor nanocavity lasers with ultralow thresholds. *Nature* **2015**, *520*, 69−U142.

(6) Hill, M. T.; Oei, Y. S.; Smalbrugge, B.; Zhu, Y.; De Vries, T.; Van Veldhoven, P. J.; Van Otten, F. W. M.; Eijkemans, T. J.; Turkiewicz, J. P.; De Waardt, H.; Geluk, E. J.; Kwon, S. H.; Lee, Y. H.; Notzel, R.;

DOI: 10.1021/acsphotonics.7b00010
ACS Photonics 2017, 4, 674−680

Smit, M. K. Lasing in metallic- Coated nanocavities. *Nat. Photonics* **2007**, *1*, 589−594.
(7) Oulton, R. F.; Sorger, V. J.; Zentgraf, T.; Ma, R.-M.; Gladden, C.; Dai, L.; Bartal, G.; Zhang, X. Plasmon lasers at deep subwavelength scale. *Nature* **2009**, *461*, 629−632.
(8) Born, M.; Wolf, E. *Principles of Optics Electromagnetic Theory of Propagation Interference and Diffraction of Light*, 7th ed.; Cambridge University Press: New York, 1999.
(9) Gramotnev, D. K.; Bozhevolnyi, S. I. Plasmonics beyond the diffraction limit. *Nat. Photonics* **2010**, *4*, 83−91.
(10) Bergman, D. J.; Stockman, M. I. Surface plasmon amplification by stimulated emission of radiation: quantum generation of coherent surface plasmons in nanosystems. *Phys. Rev. Lett.* **2003**, *90*, 027402.
(11) Purcell, E. M. Spontaneous emission probabilities at radio frequencies. *Phys. Rev.* **1946**, *69*, 681.
(12) Van Exter, M.; Nienhuis, G.; Woerdman, J. Two simple expressions for the spontaneous emission factor β. *Phys. Rev. A: At., Mol., Opt. Phys.* **1996**, *54*, 3553.
(13) Hill, M. T.; Marell, M.; Leong, E. S.; Smalbrugge, B.; Zhu, Y.; Sun, M.; van Veldhoven, P. J.; Geluk, E. J.; Karouta, F.; Oei, Y.-S. Lasing in metal-insulator-metal sub-wavelength plasmonic waveguides. *Opt. Express* **2009**, *17*, 11107−11112.
(14) Kwon, S.-H.; Kang, J.-H.; Seassal, C.; Kim, S.-K.; Regreny, P.; Lee, Y.-H.; Lieber, C. M.; Park, H.-G. Subwavelength plasmonic lasing from a semiconductor nanodisk with silver nanopan cavity. *Nano Lett.* **2010**, *10*, 3679−3683.
(15) Noginov, M.; Zhu, G.; Belgrave, A.; Bakker, R.; Shalaev, V.; Narimanov, E.; Stout, S.; Herz, E.; Suteewong, T.; Wiesner, U. Demonstration of a spaser-based nanolaser. *Nature* **2009**, *460*, 1110−1112.
(16) Meng, X.; Guler, U.; Kildishev, A. V.; Fujita, K.; Tanaka, K.; Shalaev, V. M. Unidirectional spaser in symmetry-broken plasmonic core-shell nanocavity. *Sci. Rep.* **2013**, *3*.10.1038/srep01241
(17) van Beijnum, F.; van Veldhoven, P. J.; Geluk, E. J.; de Dood, M. J.; Gert, W.; van Exter, M. P. Surface plasmon lasing observed in metal hole arrays. *Phys. Rev. Lett.* **2013**, *110*, 206802.
(18) Zhou, W.; Dridi, M.; Suh, J. Y.; Kim, C. H.; Co, D. T.; Wasielewski, M. R.; Schatz, G. C.; Odom, T. W. Lasing action in strongly coupled plasmonic nanocavity arrays. *Nat. Nanotechnol.* **2013**, *8*, 506−511.
(19) Meng, X.; Liu, J.; Kildishev, A. V.; Shalaev, V. M. Highly directional spaser array for the red wavelength region. *Laser Photon. Rev.* **2014**, *8*, 896−903.
(20) Slobozhanyuk, A. P.; Ginzburg, P.; Powell, D. A.; Iorsh, I.; Shalin, A. S.; Segovia, P.; Krasavin, A. V.; Wurtz, G. A.; Podolskiy, V. A.; Belov, P. A. Purcell effect in hyperbolic metamaterial resonators. *Phys. Rev. B: Condens. Matter Mater. Phys.* **2015**, *92*, 195127.
(21) Shalaginov, M. Y.; Vorobyov, V. V.; Liu, J.; Ferrera, M.; Akimov, A. V.; Lagutchev, A.; Smolyaninov, A. N.; Klimov, V. V.; Irudayaraj, J.; Kildishev, A. V. Enhancement of single-photon emission from nitrogen-vacancy centers with TiN/(Al, Sc)N hyperbolic metamaterial. *Laser Photon. Rev.* **2015**, *9*, 120−127.
(22) Lu, D.; Kan, J. J.; Fullerton, E. E.; Liu, Z. Enhancing spontaneous emission rates of molecules using nanopatterned multilayer hyperbolic metamaterials. *Nat. Nanotechnol.* **2014**, *9*, 48−53.
(23) Elser, J.; Wangberg, R.; Podolskiy, V. A.; Narimanov, E. E. Nanowire metamaterials with extreme optical anisotropy. *Appl. Phys. Lett.* **2006**, *89*, 261102.
(24) Jacob, Z.; Alekseyev, L. V.; Narimanov, E. Optical hyperlens: far-field imaging beyond the diffraction limit. *Opt. Express* **2006**, *14*, 8247−8256.
(25) Drachev, V. P.; Podolskiy, V. A.; Kildishev, A. V. Hyperbolic metamaterials: new physics behind a classical problem. *Opt. Express* **2013**, *21*, 15048−15064.
(26) Poddubny, A.; Iorsh, I.; Belov, P.; Kivshar, Y. Hyperbolic metamaterials. *Nat. Photonics* **2013**, *7*, 948−957.
(27) Smith, D. R.; Schurig, D. Electromagnetic wave propagation in media with indefinite permittivity and permeability tensors. *Phys. Rev. Lett.* **2003**, *90*, 077405.
(28) Cortes, C. L.; Newman, W.; Molesky, S.; Jacob, Z. Quantum nanophotonics using hyperbolic metamaterials. *J. Opt.* **2012**, *14*, 063001.
(29) Garnett, J. C. M. Colours in metal glasses, in metallic films, and in metallic solutions. II. *Philos. Trans. R. Soc., A* **1906**, *205*, 237−288.
(30) Liu, Y.; Bartal, G.; Zhang, X. All-angle negative refraction and imaging in a bulk medium made of metallic nanowires in the visible region. *Opt. Express* **2008**, *16*, 15439−15448.
(31) Noginov, M.; Barnakov, Y. A.; Zhu, G.; Tumkur, T.; Li, H.; Narimanov, E. Bulk photonic metamaterial with hyperbolic dispersion. *Appl. Phys. Lett.* **2009**, *94*, 151105.
(32) Wells, B. M.; Zayats, A. V.; Podolskiy, V. A. Nonlocal optics of plasmonic nanowire metamaterials. *Phys. Rev. B: Condens. Matter Mater. Phys.* **2014**, *89*, 035111.
(33) Vasilantonakis, N.; Nasir, M. E.; Dickson, W.; Wurtz, G. A.; Zayats, A. V. Bulk plasmon-polaritons in hyperbolic nanorod metamaterial waveguides. *Laser Photon. Rev.* **2015**, *9*, 345−353.
(34) Tsai, K.-T.; Wurtz, G. A.; Chu, J.-Y.; Cheng, T.-Y.; Wang, H.-H.; Krasavin, A. V.; He, J.-H.; Wells, B. M.; Podolskiy, V. A.; Wang, J.-K. Looking into meta-atoms of plasmonic nanowire metamaterial. *Nano Lett.* **2014**, *14*, 4971−4976.
(35) Kabashin, A.; Evans, P.; Pastkovsky, S.; Hendren, W.; Wurtz, G.; Atkinson, R.; Pollard, R.; Podolskiy, V.; Zayats, A. Plasmonic nanorod metamaterials for biosensing. *Nat. Mater.* **2009**, *8*, 867−871.
(36) Dickson, W.; Beckett, S.; McClatchey, C.; Murphy, A.; O'Connor, D.; Wurtz, G. A.; Pollard, R.; Zayats, A. V. Hyperbolic polaritonic crystals based on nanostructured nanorod metamaterials. *Adv. Mater.* **2015**, *27*, 5974−5980.
(37) Yao, J.; Liu, Z.; Liu, Y.; Wang, Y.; Sun, C.; Bartal, G.; Stacy, A. M.; Zhang, X. Optical negative refraction in bulk metamaterials of nanowires. *Science* **2008**, *321*, 930−930.
(38) Naik, G. V.; Liu, J.; Kildishev, A. V.; Shalaev, V. M.; Boltasseva, A. Demonstration of Al: ZnO as a plasmonic component for near-infrared metamaterials. *Proc. Natl. Acad. Sci. U. S. A.* **2012**, *109*, 8834−8838.
(39) Naik, G. V.; Saha, B.; Liu, J.; Saber, S. M.; Stach, E. A.; Irudayaraj, J. M.; Sands, T. D.; Shalaev, V. M.; Boltasseva, A. Epitaxial superlattices with titanium nitride as a plasmonic component for optical hyperbolic metamaterials. *Proc. Natl. Acad. Sci. U. S. A.* **2014**, *111*, 7546−7551.
(40) Tumkur, T.; Gu, L.; Kitur, J.; Narimanov, E. E.; Noginov, M. Control of absorption with hyperbolic metamaterials. *Appl. Phys. Lett.* **2012**, *100*, 161103.
(41) Belov, P.; Marques, R.; Maslovski, S.; Nefedov, I.; Silveirinha, M.; Simovski, C.; Tretyakov, S. Strong spatial dispersion in wire media in the very large wavelength limit. *Phys. Rev. B: Condens. Matter Mater. Phys.* **2003**, *67*, 113103.
(42) Fang, A.; Koschny, T.; Soukoulis, C. M. Optical anisotropic metamaterials: Negative refraction and focusing. *Phys. Rev. B: Condens. Matter Mater. Phys.* **2009**, *79*, 245127.
(43) Guo, Y.; Cortes, C. L.; Molesky, S.; Jacob, Z. Broadband super-Planckian thermal emission from hyperbolic metamaterials. *Appl. Phys. Lett.* **2012**, *101*, 131106.
(44) Ferrari, L.; Lu, D.; Lepage, D.; Liu, Z. Enhanced spontaneous emission inside hyperbolic metamaterials. *Opt. Express* **2014**, *22*, 4301−4306.
(45) Liu, Z.; Lee, H.; Xiong, Y.; Sun, C.; Zhang, X. Far-field optical hyperlens magnifying sub-diffraction-limited objects. *Science* **2007**, *315*, 1686−1686.
(46) Noginov, M.; Mozafari, A.; Tumkur, T.; Kitur, J.; Narimanov, E. Thermal radiation of lamellar metal-dielectric metamaterials and metallic surfaces. *Opt. Mater. Express* **2015**, *5*, 1511−1525.
(47) Kim, J.; Drachev, V. P.; Jacob, Z.; Naik, G. V.; Boltasseva, A.; Narimanov, E. E.; Shalaev, V. M. Improving the radiative decay rate for dye molecules with hyperbolic metamaterials. *Opt. Express* **2012**, *20*, 8100−8116.

DOI: 10.1021/acsphotonics.7b00010
ACS Photonics 2017, 4, 674−680

(48) Jacob, Z.; Kim, J.-Y.; Naik, G. V.; Boltasseva, A.; Narimanov, E. E.; Shalaev, V. M. Engineering photonic density of states using metamaterials. *Appl. Phys. B: Lasers Opt.* **2010**, *100*, 215−218.
(49) Noginov, M.; Li, H.; Barnakov, Y. A.; Dryden, D.; Nataraj, G.; Zhu, G.; Bonner, C.; Mayy, M.; Jacob, Z.; Narimanov, E. Controlling spontaneous emission with metamaterials. *Opt. Lett.* **2010**, *35*, 1863−1865.
(50) Krishnamoorthy, H. N.; Jacob, Z.; Narimanov, E.; Kretzschmar, I.; Menon, V. M. Topological transitions in metamaterials. *Science* **2012**, *336*, 205−209.
(51) Galfsky, T.; Krishnamoorthy, H.; Newman, W.; Narimanov, E.; Jacob, Z.; Menon, V. Active hyperbolic metamaterials: enhanced spontaneous emission and light extraction. *Optica* **2015**, *2*, 62−65.
(52) Shalaginov, M. Y.; Ishii, S.; Liu, J.; Irudayaraj, J.; Lagutchev, A.; Kildishev, A. V.; Shalaev, V. M. Broadband enhancement of spontaneous emission from nitrogen-vacancy centers in nanodiamonds by hyperbolic metamaterials. *Appl. Phys. Lett.* **2013**, *102*, 173114.
(53) Kitur, J. K.; Gu, L.; Tumkur, T.; Bonner, C.; Noginov, M. A. Stimulated emission of surface plasmons on top of metamaterials with hyperbolic dispersion. *ACS Photonics* **2015**, *2*, 1019−1024.
(54) Moon, J.-M.; Wei, A. Uniform gold nanorod arrays from polyethylenimine-coated alumina templates. *J. Phys. Chem. B* **2005**, *109*, 23336−23341.
(55) Moon, J.-M.; Wei, A. Controlled Growth of Gold Nanorod Arrays from Polyethylenimine-Coated Alumina Templates. *MRS Online Proc. Libr.* **2006**, *900E*, O.12.32−112.32−7.
(56) Starko-Bowes, R.; Atkinson, J.; Newman, W.; Hu, H.; Kallos, T.; Palikaras, G.; Fedosejevs, R.; Pramanik, S.; Jacob, Z. Optical characterization of epsilon-near-zero, epsilon-near-pole, and hyperbolic response in nanowire metamaterials. *J. Opt. Soc. Am. B* **2015**, *32*, 2074−2080.
(57) Novotny, L.; Hecht, B. *Principles of Nano-optics*; Cambridge University Press, 2012.
(58) Meng, X. G.; Kildishev, A. V.; Fujita, K.; Tanaka, K.; Shalaev, V. M. Wavelength-Tunable Spasing in the Visible. *Nano Lett.* **2013**, *13*, 4106−4112.
(59) Yang, A. K.; Li, Z. Y.; Knudson, M. P.; Hryn, A. J.; Wang, W. J.; Aydin, K.; Odom, T. W. Unidirectional Lasing from Template-Stripped Two-Dimensional Plasmonic Crystals. *ACS Nano* **2015**, *9*, 11582−11588.
(60) Kaminow, I. P.; Stulz, L. W.; Chandross, E. A.; Pryde, C. A. Photobleaching of Organic Laser Dyes in Solid Matrices. *Appl. Opt.* **1972**, *11*, 1563−1567.
(61) Amatguerri, F.; Costela, A.; Figuera, J. M.; Florido, F.; Sastre, R. Laser Action from Rhodamine 6g-Doped Poly(2-Hydroxyethyl Methacrylate) Matrices with Different Cross-Linking Degrees. *Chem. Phys. Lett.* **1993**, *209*, 352−356.
(62) Wang, Z. X.; Meng, X. G.; Choi, S. H.; Knitter, S.; Kim, Y. L.; Cao, H.; Shalaev, V. M.; Boltasseva, A. Controlling Random Lasing with Three-Dimensional Plasmonic Nanorod Metamaterials. *Nano Lett.* **2016**, *16*, 2471−2477.
(63) Cao, H.; Zhao, Y. G.; Ho, S. T.; Seelig, E. W.; Wang, Q. H.; Chang, R. P. H. Random laser action in semiconductor powder. *Phys. Rev. Lett.* **1999**, *82*, 2278−2281.
(64) Tumkur, T. U.; Kitur, J. K.; Bonner, C. E.; Poddubny, A. N.; Narimanov, E. E.; Noginov, M. A. Control of Förster energy transfer in the vicinity of metallic surfaces and hyperbolic metamaterials. *Faraday Discuss.* **2015**, *178*, 395−412.

DOI: 10.1021/acsphotonics.7b00010
ACS Photonics 2017, 4, 674−680